Research Article

Carla Giometti França, Krissia Caroline Leme, Ângela Cristina Malheiros Luzo, Jacobo Hernandez-Montelongo*, and Maria Helena Andrade Santana

Oxidized hyaluronic acid/adipic acid dihydrazide hydrogel as cell microcarriers for tissue regeneration applications

https://doi.org/10.1515/epoly-2022-0086
received August 07, 2022; accepted October 30, 2022

Abstract: Hyaluronic acid (HA) is a biopolymer present in various human tissues, whose degradation causes tissue damage and diseases. The oxidized hyaluronic acid/adipic acid dihydrazide (oxi-HA/ADH) hydrogels have attracted attention due to their advantages such as thermosensitivity, injectability, *in situ* gelation, and sterilization. However, studies are still scarce in the literature as microcarriers. In that sense, this work is a study of oxi-HA/ADH microparticles of 215.6 ± 2.7 μm obtained by high-speed shearing (18,000 rpm at pH 7) as cell microcarriers. Results showed that BALB/c 3T3 fibroblasts and adipose mesenchymal stem cells (h-AdMSC) cultured on the oxi-HA/ADH microcarriers presented a higher growth of both cells in comparison with the hydrogel. Moreover, the extrusion force of oxi-HA/ADH microparticles was reduced by 35% and 55% with the addition of 25% and 75% HA fluid, respectively, thus improving its injectability. These results showed that oxi-HA/ADH microcarriers can be a potential injectable biopolymer for tissue regeneration applications.

Keywords: oxidized hyaluronic acid, adipic dihydrazide, hydrogel microcarriers, injectability, tissue engineering

*** Corresponding author: Jacobo Hernandez-Montelongo,** Department of Mathematical and Physical Sciences, Catholic University of Temuco, 4813302, Temuco, Chile, e-mail: jacobo.hernandez@uct.cl
Carla Giometti França, Maria Helena Andrade Santana: Department of Materials and Bioprocess Engineering, School of Chemical Engineering, University of Campinas, 13083-852, Campinas, SP, Brazil
Krissia Caroline Leme, Ângela Cristina Malheiros Luzo: Haematology & Hemotherapy Center, Umbilical Cord Blood Bank, University of Campinas, 13083-878, Campinas, SP, Brazil

1 Introduction

In the last few decades, minimally invasive protocols with autologous cells or exogenous products containing cultivated mesenchymal stem cells (MSCs) have been used to treat musculoskeletal diseases (1–3). Moreover, cultured fibroblasts have repaired burnt tissues and wounds that can undergo regeneration by MSCs (4–6). Natural polymer-based hydrogels have been widely investigated for applications in the fields of tissue engineering and regenerative medicine. These hydrogels must mimic the structural support of the native extracellular matrix and allow three-dimensional attachment, migration proliferation, or additional differentiation of incorporated cells (7–10).

Hyaluronic acid (HA) is a biopolymer abundant in various tissues, especially in cartilage and skin. Exogenous HA, obtained from microbial fermentation, exhibits the same properties as the endogenous HA and has been widely used for tissue repair and regeneration (11–15). Moreover, external HA reposition has been used as an effective therapeutic target in human diseases (16). The highly hydrated structure of HA, its viscoelastic and viscous properties benefit boundary lubrication, shock absorption, and viscosupplementation. These are reasons for the extensive use of HA to restore the functions of the synovial fluid and damaged cartilage. Furthermore, signalization via cell receptors produces anti-inflammatory effects, pain relief, protection, and restoration of the chondral matrix make HA a disease modifier in osteoarthritis (17–19).

Thus, HA and its synthetic derivatives mimic the natural physical and structural environment in the living tissue (20–23). Due to its properties, HA injections with MSCs in damaged sites promote pain relief, tissue repair, or regeneration (24,25). Although there is an extensive use of exogenous HA in musculoskeletal diseases, improvements in functionality need to be confirmed. The flexibility of HA molecular groups for chemical modifications, including crosslinking, increases its stability and expands

its uses as a vehicle for drug delivery or as cell-laden (26,27). Therefore, new strategies have been investigated to improve the therapeutic applications of HA.

The partial oxidation of its hydroxyl groups by sodium periodate introduces highly flexible links causing structural and rheological changes compared to non-oxidized HA. Furthermore, the partial oxidation allows crosslinking with small molecules such as adipic acid dihydrazide (ADH), a metabolized crosslinker, by click reaction type (20,28). The oxidized hyaluronic acid/adipic acid dihydrazide (oxi-HA/ADH) hydrogels have attracted attention due to lower viscosity and improved injectability, biocompatibility, thermosensitivity, and *in situ* gelation than HA. Although there are still a few studies, oxi-HA/ADH hydrogels carrying cells could be promising for nucleus pulposus regeneration (11), post epidural fibrosis surgery (29), as a drug carrier (30), and with dual effects (drug delivery and regeneration) in tendinopathies (31). Moreover, studies associating structural properties and biological performance as a cell microcarrier are still scarce in the literature, despite this type of materials can effectively promote the growth of cells. For example, Jui-Yang La obtained functionalized gelatin microparticles with oxi-HA for corneal cells' culture (32,33). This is a potential application because HA does not present enough stability in simulated body fluids (20). To reduce its degradation degree, chemical modifications are necessary, in that sense, when HA is oxidized and crosslinked with ADH, a stable hydrogel is achieved with promising applications as a cell microcarrier. Previous studies of our group investigated the colloidal structural changes on oxi-HA and modulation of physicochemical properties of oxi-HA/ADH hydrogels with the oxidation degree and ADH concentration (20), and its use as controlled drug delivery when combined with microparticles of nanoporous silicon (34).

Thus, in this study, we prepared the oxi-HA/ADH as the whole hydrogel and as microcarriers to investigate the influence of their structure on cell association of fibroblast and MSC proliferation. The cell association inside or outside the whole hydrogel or on the surface of microcarriers could represent top-down and bottom-up approaches to the potential formation of microtissues. The structuring of oxi-HA/ADH in microcarriers enables the increase of the surface area for cell adhesion, contributing to proliferation. Moreover, we also analyzed the effects of the injectability alone or mixed with non-oxidized HA. Therefore, the innovation of this work is synthesis of oxi-HA/ADH microparticles by high-speed shearing, and their study as potential cell microcarriers for tissue regeneration compared with oxi-HA/ADH as a whole hydrogel. We consider that these aspects are the starting point for further studies on mechanisms involving oxi-HA/ADH and cells.

2 Materials and methods

2.1 Materials and reagents

HA with an average molecular weight of 8.54×10^5 Da was purchased from Tops Shandong Topscience Biotech Co. (Rizhao, CH). Sodium periodate ($NaIO_4$), ethylene glycol, ADH, and sodium bicarbonate ($NaHCO_3$) were purchased from Sigma-Aldrich Inc. (St Louis, MO, USA). Phosphate buffered saline (PBS) was supplied by Laborclin Ltda (Pinhais, Paraná, BR). Dialysis membranes with a nominal molecular weight cutoff (MWCO) of 12,000–16,000 Da were sourced from Inlab (Diadema, São Paulo, BR). Fetal bovine serum (FBS) and penicillin–streptomycin were purchased from Thermo Fisher Scientific (Waltham, Massachusetts, USA).

The stock cultures of BALB/c 3T3 mouse fibroblasts (American Type Culture Collection – ATCC-CCL163) were provided by Sigma-Aldrich Inc. (St Louis, MO, USA). The human adipose-derived mesenchymal stem cells (h-AdMSCs) were isolated from the human subcutaneous adipose tissue of patients undergoing lipo-aspiration at the University Hospital and isolated and cultured according to a previous protocol (20).

2.2 Methods

2.2.1 Preparation of oxi-HA

Oxi-HA was synthesized according to the reported procedure (17,35) with modifications. HA with a concentration of 1% (w/v) was dissolved in double-distilled water at room temperature, and then an aqueous periodate ($NaIO_4$) solution (10.67%, w/v) was added. The reaction occurred at room temperature for 24 h in a dark environment. The $NaIO_4$:HA ratio was calculated as $NaIO_4$ mol per HA dimer mol. The reaction was stopped by the addition of ethylene glycol for half an hour. The molar ratio of ethylene glycol to $NaIO_4$ was 1:6. The resulting solution was dialyzed with double-distilled water for 3 days using a semipermeable membrane (with an MWCO of 12,000–16,000 Da). Finally, the dialyzed solution was lyophilized, yielding a white fluffy product.

2.2.2 Preparation of the substrates

2.2.2.1 Preparation of the oxi-HA/ADH hydrogel

The oxi-HA/ADH hydrogel was obtained according to França et al. (20). Briefly, oxi-HA with a degree of oxidation 65% was dissolved in a PBS (pH of 7.4, at 4°C) to obtain a final concentration of 6% (w/v). Then, an 8% (w/v) ADH solution was also prepared in PBS at 4°C. The oxi-HA and ADH solutions were mixed in Eppendorf tubes at a volume ratio of 4:1 oxi-HA/ADH (400 mL of oxi-HA/100 mL of ADH). The Eppendorf tubes were submerged in a bath at 0°C for 10 min to obtain the oxi-HA/ADH hydrogel.

2.2.2.2 Preparation of the oxi-HA/ADH microcarriers

To achieve the oxi-HA/ADH microcarriers, one of the oxi-HA/ADH hydrogels obtained in the previous section was immersed in ultrapure water at pH 7 and was submitted to high-speed shearing in an Ultra-Turrax® T25 homogenizer (IKA Labortechnik, Germany) for 10 min using a shear rate of 18,000 rpm. Afterward, the solution was centrifuged to separate the oxi-HA/ADH microcarriers by decantation.

2.2.3 Physicochemical characterizations

The morphologies of the oxi-HA/ADH hydrogel and microcarriers were obtained by scanning electron microscopy (SEM) (LEO 440i, Cambridge, England) using a current and voltage of 50 pA and 10 kV, respectively. The average pores sizes of the hydrogel were determined by measuring 100 individual pores from three different images using ImageJ software. The porosity of the oxi-HA/ADH hydrogel was measured in a 20 mL volumetric flask using the procedure according to Zu et al. (36):

$$\text{Porosity (\%)} = 100 \cdot \left(\frac{V_p}{V_p + V_g} \right) \quad (1)$$

where V_p is the volume of cyclohexane, an inert solvent, in the pore (cm^3) and V_g is the volume of the hydrogel (cm^3).

The chemical analysis of the oxi-HA/ADH hydrogel was performed by Attenuated Total Reflectance Fourier-Transform Infra-Red Spectroscopy (ATR-FTIR). An FTIR spectrometer (CARY 630 FTIR Agilent Technologies, USA) was used in a range between 4,000 and 600 cm^{-1} with a resolution of 1 cm^{-1} (NS = 4). Moreover, the mean diameter of the oxi-HA/ADH microcarriers was performed by laser scattering in a Mastersizer-S (Malvern Instruments, UK). The particle size analysis was performed with the hydrogels dispersed in water. The standard deviation was calculated from ten measurements of the mean diameter. The zeta potential of both kinds of samples was measured by a ZetaSizer Nano–ZS (Malvern Ltd, Royston, UK) in distilled water.

2.2.4 Cell culture studies

2.2.4.1 BALB/c 3T3 culture

The BALC/c 3T3 mouse fibroblast cells were grown in plastic flasks (75 cm^2) with Dulbecco's modified Eagle medium (DMEM), supplemented with 10% inactivated FBS and 1% antibiotic solution penicillin–streptomycin–amphotericin (PSA). The cultures were incubated at 37°C in an atmosphere containing 5% CO_2. The medium was changed every 72 h, and when the culture reached confluence, the subculture was treated with trypsin-EDTA, until the complete release of the cells. Cells from passages 4–6 were trypsinized and seeded in hydrogel (inside or outside) at a concentration of 1×10^4 cells/well (well of 1.1 cm^2). For seeding cells inside the hydrogel, cells were mixed with the ADH solution before mixing both the solutions (300 mL of oxi-HA/ADH solution/well), then, the solutions were mixed and the gelation at 0°C for 10 min was performed according to Section 2.2.2. For seeding cells outside the hydrogel, cells were cultured on the surface of the oxi-HA/ADH hydrogel after the gelation was obtained from 300 mL of oxi-HA/ADH solution/well. For the microcarriers, cells were seeded on the surface of the microcarriers at a concentration of 2×10^4 cells/well (well of 1.1 cm^2). Micro-hydrogel particles were obtained from a 300 mL of oxi-HA/ADH solution. After adhesion, 700 µL of high-glucose DMEM (Thermo Fisher Scientific, Waltham, MA, USA) was added to the wells, and cells were cultured in a humidified incubator at 37°C and 5% CO_2 with the medium changed every 3 days. The experiment was performed in triplicate ($n = 3$) for each group.

2.2.4.2 h-AdMSC culture

The h-AdMSCs were cultured in DMEM, containing 15 mM HEPES buffer, L-glutamine, pyridoxine hydrochloride, 3.7 g $NaHCO_3$, and supplemented with 10% FBS and 1% PSA. Cells from passages 4–6 were trypsinized and seeded in

microcarrier at a concentration of 2×10^4 cells/well. After adhesion, 700 µL of low-glucose DMEM (Thermo Fisher Scientific, Waltham, MA, USA) was added to the wells, and cells were cultured in a humidified incubator at 37°C and 5% CO_2 with the medium changed every 3 days. The experiment was performed in triplicate (n = 3) for each group.

2.2.4.3 Cytotoxicity assays

For cytotoxicity assays, BALB/c 3T3 cells were distributed in 24-well plates using a density of 5×10^4 cell·mL^{-1} and were incubated at 37°C at 5% CO_2 for 24 h. Later, the cells were treated with different concentrations (0–5 mg·mL^{-1}) of oxi-HA dispersion or ADH solution for 72 h. oxi-HA/ADH hydrogel was also cultured with cells for 72 h. After incubation, the medium was removed, wells were washed with PBS, and 200 µL of 3-(4,5-dimethylthiazol-2-yl)-2,5-diphenyltetrazolium bromide (MTT) solution (1 mg·mL^{-1}) was added to each well. The plate was incubated for 3 h at 37°C, MTT solution was removed, and the formazan crystal was solubilized in 1 mL of dimethyl sulfoxide (DMSO). The plate was shaken for 5 min, and the absorbance of each well was read using an Infinity M200Pro spectrophotometer (Männedorf, Switzerland). The measured absorbance at λ = 570 nm was normalized to the value obtained for the control: cells were cultured without samples (37).

2.2.4.4 BALB/c 3T3 and h-AdMSC proliferation kinetics

Cell growth was assessed by MTT (Sigma-Aldrich, St Louis, MO, USA) assays (37). Samples were incubated with MTT for 4 h at 37°C with predetermined days. Then, MTT was replaced with DMSO, the samples were left in an orbital shaker for 30 min, and the absorbance was measured at 570 nm. The experiments were conducted in triplicate (n = 3) for each group.

2.2.5 Extrusion force

The force required to extrude the hydrogels was determined by loading the hydrogels and their gel/fluid dispersions in 1 mL plastic syringes with 30-gauge needles. The measurements were performed in TA.XT.plus Texture analyzer (Stable Micro Systems, Vienna Court, UK) (load cell 50 kg) at 25°C at a 5.0 mm·min^{-1} extrusion rate.

2.2.6 Statistical analysis

Cell culture and extrusion force tests were performed in triplicate and data from each assay were analyzed statistically by analysis of variance with subsequent Tukey *post-hoc* test using the OriginLab software; p-values of 0.05 or less were considered statistically significant.

3 Results

3.1 Cytotoxicity of hydrogel precursor components

Table 1 shows the influence of the concentration of oxi-HA and ADH solutions on cell cytotoxicity as assayed by MTT. The results revealed nonpotential cytotoxicity over 3 days (72 h) for both solutions according to the standard values: cell viability was higher than half maximal inhibitory concentration (IC_{50}) in both the cases. However, there was a significant decrease in cell viability for oxi-HA dispersion at higher concentrations (above 0.5 mg·mL^{-1}). These results confirm the biocompatibility of the hydrogel precursor components.

3.2 Physicochemical characterizations of hydrogel

On the other hand, a general view of the oxi-HA/ADH hydrogel is presented in Figure 1a. The microscopic image in Figure 1b shows its internal porous structure, which presented a porosity of 67 ± 3% with a pore size of 105 ± 24 µm and a zeta potential of −36 ± 3 mV. On the other hand, Figure 1c shows the ATR-FTIR spectrum of the hydrogel. The presented bands are according to the chemical structure of oxi-HA/ADH (Figure 1d) (20,34). Bands

Table 1: Cell cytotoxicity of BALB/c 3T3 (%) exposed to oxi-HA acid and ADH solution; data are reported as mean ± SD for experiments in triplicate

Solution	Concentration (mg·mL^{-1})					
	0.0	0.25	0.5	1.0	2.5	5.0
oxi-HA	100 ± 2.5	90.2 ± 2.1	76.6 ± 2.6	76.6 ± 2.4	72.4 ± 2.6	72.8 ± 2.5
ADH	100 ± 1.5	101.2 ± 2.0	99.3 ± 2.9	98.3 ± 3.5	94.0 ± 3.0	94.2 ± 3.1

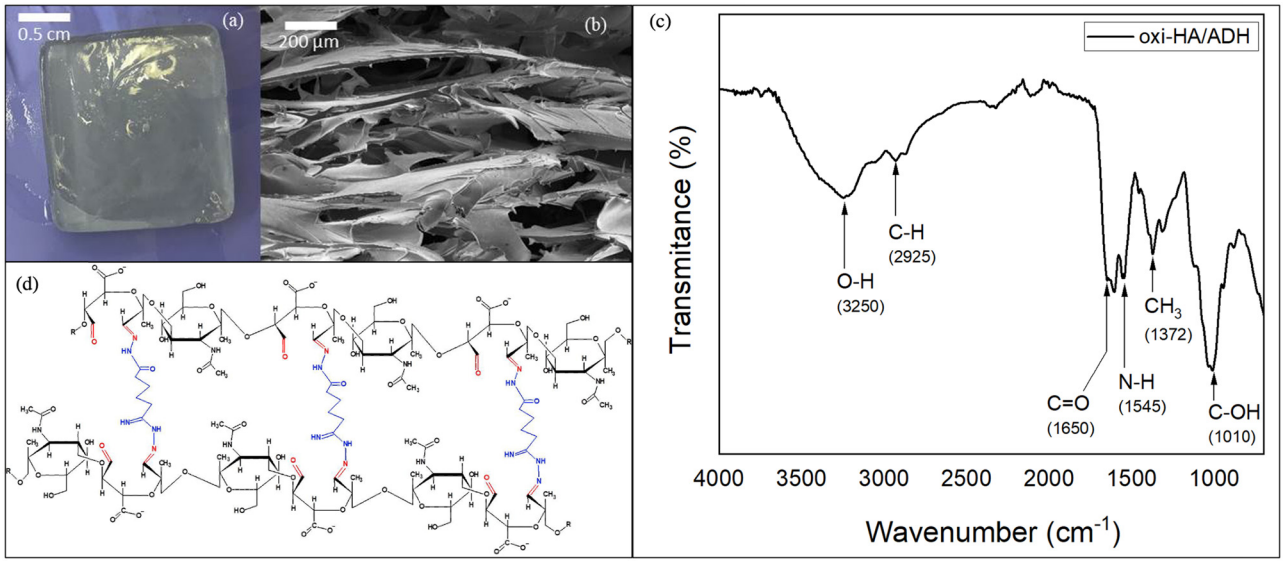

Figure 1: oxi-HA/ADH hydrogel: (a) macroscopic image, (b) surface scanning electron microscopic image, (c) ATR-FTIR spectrum, and (d) chemical structure.

were detected at 1,010, 1,372, 1,545, and 1,650 cm^{-1}, which can be attributed to the C–OH stretching mode, CH_3 symmetric bending, secondary amide N–H bending, and secondary amide C═O stretching, respectively. Moreover, the band at 2,925 cm^{-1} corresponds to C–H stretching vibration, and the wide band at 3,250 cm^{-1} is attributed to O–H stretching of the hydroxyl groups.

3.3 Cell assays in the hydrogel

Figure 2 shows the proliferation of BALB/c 3T3 cells inside and outside the hydrogel for 14 days. The viability of cells was kept inside the hydrogel because the time in oxi-HA/ADH solution is short: just 10 min of gelation, after that, the porous oxi-HA/ADH hydrogel was obtained and the culture medium was added. The results revealed nonpotential cytotoxicity over 3 days for the oxi-HA/ADH hydrogel according to the standard values (IC_{50}). Besides, the cells inside and outside the hydrogel showed growth between the third and the seventh day, while a short lag phase was observed in the absence of hydrogel after the third day. After 10 days, the cells inside and outside the oxi-HA/ADH hydrogel were in the stationary and decay phase (cell death). It is important to highlight that cell concentration reached maximum values at different times: 45,780 cells·mL^{-1} at Day 14; 31,833 cells·mL^{-1} at Day 10; and 40,100 cells·mL^{-1} at Day 3 for the cells seeded inside, outside, and the control, respectively. On the other hand, cells inside the hydrogel presented a faster doubling time of cells compared to cells outside the hydrogel because matrix promoted cell junctions, which enhance cell-to-cell communication and interaction; moreover, the porosity of hydrogel allows the diffusion of oxygen, nutrients, ions, and electrical currents (38,39).

3.4 Physicochemical characterizations of microcarriers

The oxi-HA/ADH microcarriers were obtained by ultra-turrax® shearing at 18,000 rpm and pH 7 and were characterized by the dynamic light scattering (DLS), zeta

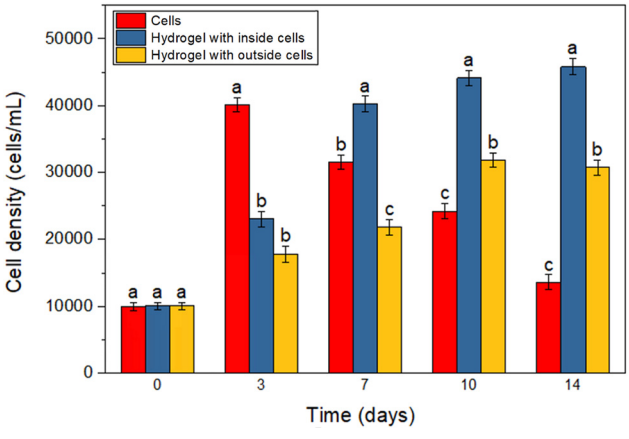

Figure 2: BALB/c 3T3 proliferation starting inside or outside the oxi-HA/ADH hydrogel during cultivation for 14 days. Data are reported as mean ± SD for experiments in triplicate. Mean values of the same group of days with the same letter indicate that there is no significant difference ($p < 0.05$) by the Tukey test.

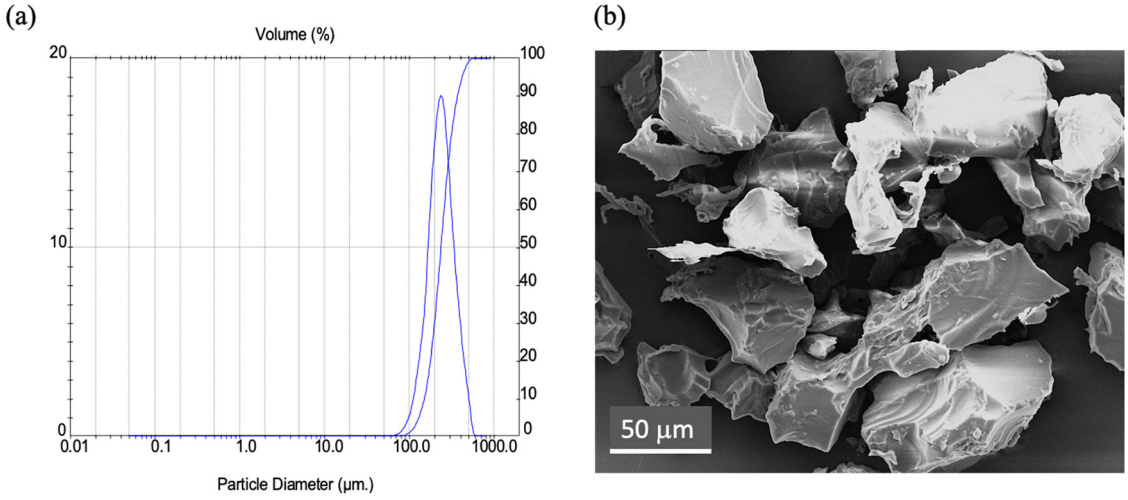

Figure 3: Microcarriers oxi-HA/ADH hydrogel as microcarriers prepared at 18,000 rpm and pH 7: (a) cumulative hydrodynamic diameter and volume distribution and (b) surface scanning electron microscopic image.

potential, and SEM techniques (Figure 3). Using the DLS, the hydrodynamic diameter and volume distribution of particles were determined (Figure 3a). The average diameter of particles was 215.6 ± 2.7 µm. The monodispersity can be explained due to the neutral pH because the structure of HA at pH 7 presents random coil conformation (40). At acidic pH, for example, HA shows a mixed structure (random coil + double helix), which could generate polydispersity. Regarding the zeta potential, microcarriers presented a value of −17.8 ± 1.9 mV. In that sense, particles could agglutinate because only particles that possess zeta potentials of more than +30 mV or less than −30 mV present enough strong repulsion forces for a good stability (41).

On the other hand, the synthetized oxi-HA/ADH microcarriers are shown in the SEM image of Figure 3b. Microparticles presented an irregular shape, a size of around 100 µm and no pores on their surface. The higher size obtained by DLS could be due to the agglutination of particles, as suggested by the zeta potential results.

3.5 Cell assays on the microcarriers

To study the oxi-HA/ADH as cell microcarriers, BALB/c 3T3 and h-AdMSC cultures were performed. Figure 4 shows the proliferation of BALB/c 3T3 (Figure 4a) and

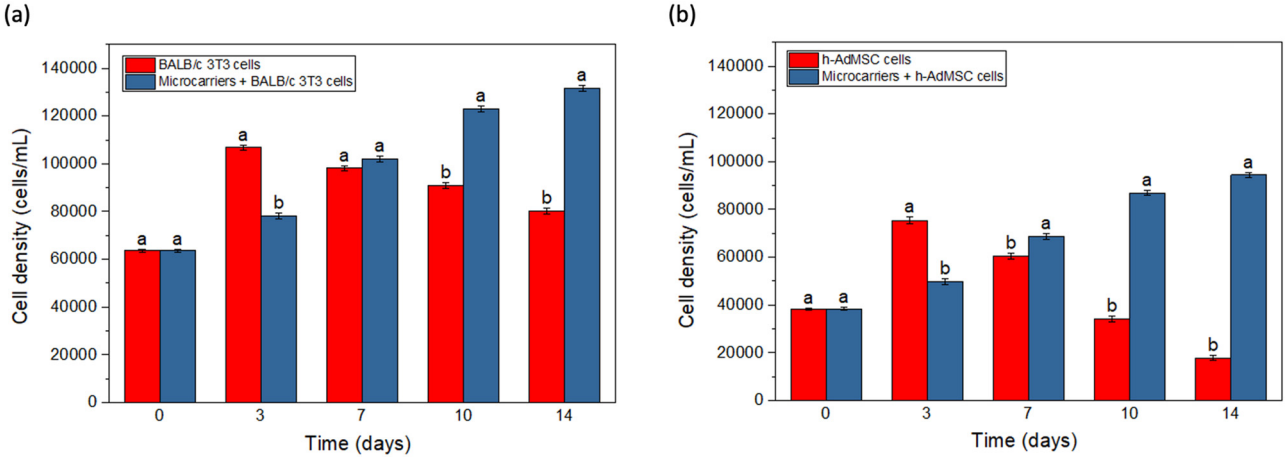

Figure 4: (a) BALB/c 3T3 and (b) h-AdMSC proliferation on the microcarriers during cultivation for 14 days in supplemented DMEM medium, assessed by MTT assay. Data are reported as mean ± SD for experiments in triplicate. Mean values of the same group of days with the same letter indicate that there is no significant difference ($p < 0.05$) by the Tukey test.

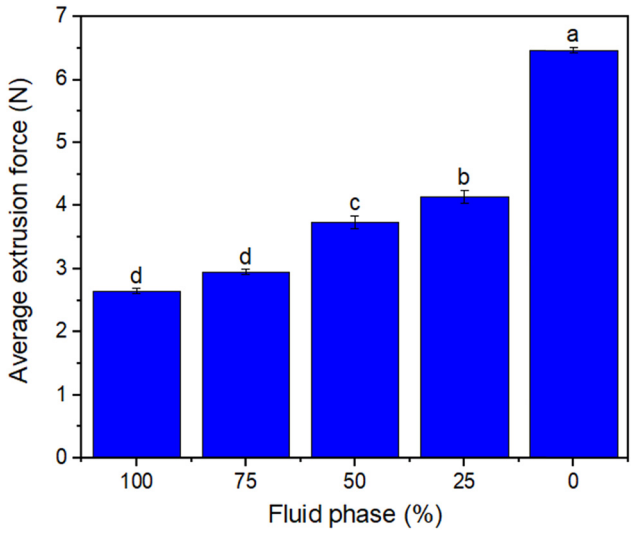

Figure 5: Influence of the fluid phase fraction of HA on the extrusion force of the oxi-HA/ADH microcarriers. Data are reported as mean ± SD for experiments in triplicate. Mean values with the same letter indicate that there is no significant difference ($p < 0.05$) by the Tukey test.

h-AdMSC (Figure 4b) cells with and without the oxi-HA/ADH microcarriers. In both cultures, although the lag phase was longer, the growth of both cells was higher on the microcarriers. This lag phase can be explained because on microcarriers a small number of cells are attached on the surface and the cell signaling could be delayed. On the other hand, h-AdMSCs without microcarrier presented a strong decay phase after Day 7, and BALB/c 3T3 cells without microcarrier showed a soft decay phase since Day 3.

3.6 Extrusion tests

Figure 5 shows the average forces required to extrude the microcarriers through a syringe equipped with a 30G½ needle. The extrusion to force pure microcarriers, without any fraction of fluid phase (HA), was around 6.5 N. However, the addition of 25% and 75% HA fluid reduced the extrusion force by 35% and 55% approximately, which avoids side effects such as pain, discomfort, bruising, bleeding, or edema (42,43).

4 Discussion

Nowadays, it is well known that HA plays an essential role in tissue repair and regeneration associated with the resident or *in vitro* cultured cells, in addition to biological components such as growth factors. HA combines beneficial properties as a scaffold for tissue engineering such as biocompatibility, chemical modifications, and biodegradability. Furthermore, chemical crosslinking promotes stability in biological medium, and surface modifications can modify cell adhesion and the regenerative potential of resident or seeded cells. The rheological properties such as injectability could benefit the applications in minimally invasive therapies.

The partial oxidation of HA and crosslinking with ADH could provide modulation of structural changes with beneficial physicochemical and rheological properties, and improving the properties of the conventional non-oxidized HA. In this work, we hypothesized that oxi-HA/ADH with controlled properties could be an effective approach for cell expansion, tissue repair, and regenerative purposes. However, partial oxidation results in reactive aldehyde groups that make ADH crosslinking feasible, while free aldehyde groups from incomplete ADH reaction can be cytotoxic to cells (44). Aldehyde-modified polymers, such as oxi-HA, also showed a dose-dependent effect on cell viability in macrophages and mesothelial cells (26–28). Therefore, we initially investigated the concentration-dependent cytotoxicity of oxi-HA and ADH (Figure 1). Although above IC 50, concentrations above 3–6% oxi-HA reduced cell viability. ADH did not present any degree of cytotoxicity in a large range of concentrations (0.1–8%), indicating that the crosslinking did not affect cell viability. Therefore, oxi-HA/ADH concentration up to 3% oxi-HA and 8% ADH minimizes cytotoxic effects. In the current study, we used 6% oxi-HA crosslinking with 8% ADH because of its advantageous physicochemical properties, as previously investigated (20).

Initially, fibroblast cultivation was performed in the oxi-HA/ADH hydrogel, with cells inside or outside hydrogel. Although the culture medium penetration inside hydrogel was limited by diffusion to the internal microporous structure, cell-seeded inside the matrix proliferated due to the high surface area of the porous structure; the hydrogel was completely covered with viable cells after 10 days in culture (Figure 2). It is important to highlight that in the beginning of the culture, the viability of cells was kept inside the hydrogel because the time in oxi-HA/ADH solution was short: just 10 min of gelation, after that, the porous oxi-HA/ADH hydrogel was obtained and the culture medium added.

Regarding incremental surface area/mass, microcarriers with the same structural properties of hydrogel were prepared and characterized (Figure 3). The high-speed

shearing method to obtain the microcarriers was not completely efficient because microparticles were irregular and tended to agglomerate at least in pairs. SEM results showed sizes around 100 μm and DLS presented a mean of 215 μm, growth of BALB/c 3T3 and h-AdMSCs was favored. Both cells on the surface of microcarriers continued to rise at a slower rate, compared to the porous hydrogel (Figure 4). But microcarriers favored a higher cell proliferation in three-dimensional layered growth and showing potential to formation constructs (microtissues) in comparison with the hydrogel.

In this context, microcarriers represent an advantageous strategy for *in vitro* expansion of cells in bioreactors for further uses in tissue repair such as wound healing. Stability was proven up to 14 days of cultivation. Recent studies compare the performance of top-down and bottom-up approaches in cell expansion and tissue formation (45). Conceptually, the bottom-up approach is based on self-assembly or guiding from smaller components or modules as building blocks for supramolecular structures. Thus, the proliferation of MSCs on the surface of microcarriers represents a bottom-up approach for tissue regeneration.

The injectability of the microcarriers containing cells is essential for therapeutic success in internal tissues such as bone or cartilage. In that sense, HA is added to reduce viscosity and injection force of microparticles. However, the oxi-HA/ADH microcarriers showed low injection force, even without mixture with the HA fluid (non-oxidized). Anyway, the mixture reduced the viscosity and injection force in all concentrations (Figure 5).

The combination of these results indicates that the microcarriers developed in this study can provide benefits for cell expansion, tissue repair, and the proliferation of MSCs for tissue regeneration. Furthermore, structuration in microcarriers represents an innovative approach for specific cell expansion in bioreactors and direct uses in tissue repair without the need for further separation. In addition, the oxi-HA/ADH microcarriers also can be used for the encapsulation of anti-oxidants for better stability (40). Further studies may investigate the cell capability for differentiation in a required tissue. Chondrogenic differentiation is ongoing in our group.

5 Conclusions

The oxi-HA and ADH are non-cytotoxic, and the oxi-HA/ADH hydrogel is an amenable environment for being used as cell-laden. However, when the size of the hydrogel is modified from a porous macroscopic substrate to microscopic non-porous particles, it improves the proliferation of BALB/c 3T3 and h-AdMSCs. The performance of the MSC proliferation on the surface of oxi-HA/ADH microcarriers represents a promising bottom-up strategy toward cell differentiation and the production of microtissues for regeneration *in vitro* or *in vivo*. Also, the improved injectability of oxi-HA/ADH microcarriers sheds light on the development of injectability formulations for minimally invasive therapies.

Acknowledgements: The authors acknowledge In Situ Cell Therapy for providing the laboratory. The authors gratefully acknowledge prof. Dr Marcelo Lancellotti and Dra. Daisy Machado for helpful assistance with fibroblasts cells.

Funding information: This study was supported by the CNPq (Conselho Nacional de Desenvolvimento Científico e Tecnológico Brasil, process 140924/2017-5), FAPESP (Fundação de Amparo à Pesquisa do Estado de São Paulo, process 2016/10132-0), and FONDECYT–Chile (Fondo Nacional de Desarrollo Científico y Tecnológico, grant number 11180395).

Author contributions: Carla Giometti França: conceptualization, methodology, data curation, formal analysis, writing – original draft; Krissia Caroline Leme: methodology, data curation, formal analysis; Ângela Cristina Malheiros Luzo: methodology, data curation, formal analysis; Jacobo Hernandez-Montelongo: formal analysis, visualization, writing – review and editing; Maria Helena Andrade Santana: conceptualization, resources, supervision, funding acquisition.

Conflict of interest: Authors state no conflict of interest.

Data availability statement: The data that support the findings of this study are available from the corresponding author upon reasonable request.

References

(1) Weis M, Shan JW, Kuhlmann M, Jungst T, Tessmar J, Groll J. Evaluation of hydrogels based on oxidized hyaluronic acid for bioprinting. Gels. 2018;4:1–8. doi: 10.3390/gels4040082.
(2) Zakrzewski W, Dobrzynski M, Szymonowicz M, Rybak Z. Stem cells: past, present, and future. Stem Cell Res Ther. 2019;10(1):1–22. doi: 10.1186/s13287-019-1165-5.
(3) Orozco L, Munar A, Soler R, Alberca M, Soler F, Huguet M, et al. Treatment of knee osteoarthritis with autologous

mesenchymal stem cells: two-year follow-up results. Transplantation. 2014;97:e66–8. doi: 10.1097/TP.0000000000000167.
(4) Catoira MC, Fusaro L, Di Francesco D, Ramella M, Boccafoschi F. Overview of natural hydrogels for regenerative medicine applications. J Mater Sci Mater Med. 2019;30(10):1–10. doi: 10.1007/s10856-019-6318-7.
(5) Metcalfe AD, Ferguson MWJ. Tissue engineering of replacement skin: the crossroads of biomaterials, wound healing, embryonic development, stem cells and regeneration. J R Soc Interface. 2007;4:413–37. doi: 10.1098/rsif.2006.0179.
(6) Shpichka A, Butnaru D, Bezrukov EA, Sukhanov RB, Atala A, Burdukovskii V, et al. Skin tissue regeneration for burn injury. Stem Cell Res Ther. 2019;10:1–16. doi: 10.1186/s13287-019-1203-3.
(7) Wei Z, Yang JH, Liu ZQ, Xu F, Zhou JX, Zrinyi M, et al. Novel biocompatible polysaccharide-based self-healing hydrogel. Adv Funct Mater. 2015;25:1352–9. doi: 10.1002/adfm.201401502.
(8) Cerqueira MT, Marques AP, Reis RL. Using stem cells in skin regeneration: possibilities and reality. Stem Cell Dev. 2012;21:1201–14. doi: 10.1089/scd.2011.0539.
(9) Tibbitt MW, Anseth KS. Hydrogels as extracellular matrix mimics for 3D cell culture. Biotechnol Bioeng. 2009;103:655–63. doi: 10.1002/bit.22361.
(10) Fan D, Staufer U, Accardo A. Engineered 3D polymer and hydrogel microenvironments for cell culture applications. Bioengineering. 2019;6:1–43. doi: 10.3390/bioengineering6040113.
(11) Su WY, Chen YC, Lin FH. Injectable oxidized hyaluronic acid/adipic acid dihydrazide hydrogel for nucleus pulposus regeneration. Acta Biomater. 2010;6:3044–55. doi: 10.1016/j.actbio.2010.02.037.
(12) Shoham N, Sasson AL, Lin FH, Benayahu D, Haj-Ali R, Gefen A. A multiscale modeling framework for studying the mechanobiology of sarcopenic obesity. J Mech Behav Biomed Mat. 2013;28:320–31. doi: 10.1007/s10237-016-0816-z.
(13) Su WY, Chen KH, Chen YC, Lee YH, Tseng CL, Lin FH. An injectable oxidated hyaluronic acid/adipic acid dihydrazide hydrogel as a vitreous substitute. J. Biomater. Sci. Polym Ed. 2011;22:1777–97. doi: 10.1163/092050610X522729.
(14) Pouyani T, Prestwich GD. Functionalized derivatives of hyaluronic acid oligosaccharides: drug carriers and novel biomaterials. Bioconjug Chem. 1994;5(4):339–47. doi: 10.1021/bc00028a010.
(15) Fong ELS, Chan CK, Goodman SB. Stem cell homing in musculoskeletal injury. Biomaterials. 2011;32:395–409. doi: 10.1016/j.biomaterials.2010.08.101.
(16) Liang J, Jiang D, Noble PW. Hyaluronan as a therapeutic target in human diseases. Adv Drug Deliv Rev. 2016;1(97):186–203. doi: 10.1016/j.addr.2015.10.017.
(17) Lin FH, Su WY, Chen YC, Chen KH. Cross-linked oxidated hyaluronic acid for use as vitreous substitute. Patent No. 8. 197, Washington, DC: U.S. Patent and Trademark Office; 2012. p. 849.
(18) Nicholls MA, Fierlinger A, Niazi F, Bhandari M. The disease-modifying effects of hyaluronan in the osteoarthritic disease state. Clin Med Insights Arthritis Musculoskelet Disord. 2017;10:1–10. doi: 10.1177/1179544117723611.
(19) Gupta RC, Lall R, Srivastava A, Sinha A. Hyaluronic acid: molecular mechanisms and therapeutic trajectory. Front Vet Sci. 2019;6(192):1–24. doi: 10.3389/fvets.2019.00192.
(20) França CG, Sacomani DP, Villalva DG, Nascimento VF, Dávila JL, Santana MHA. Structural changes and crosslinking modulated functional properties of oxi-HA/ADH hydrogels useful for regenerative purposes. Eur Polym J. 2019;121(109288):1–11. doi: 10.1016/j.eurpolymj.2019.109288.
(21) Fallacara A, Baldini E, Manfredini S, Vertuani S. Hyaluronic acid in the third millennium. Polymers. 2018;10(7):701. doi: 10.3390/polym10070701.
(22) Knopf-Marques H, Pravda M, Wolfova L, Velebny V, Schaaf P, Vrana NE, et al. Hyaluronic Acid and its derivatives in coating and delivery systems: applications in tissue engineering, regenerative medicine and immunomodulation. Adv Healthc Mater. 2016;5:2841–55. doi: 10.1002/adhm.201600316.
(23) Menaa F, Menaa A, Menaa B. Hyaluronic acid and derivatives for tissue engineering. J Biotechnol Biomater. 2011;S1:1–7. doi: 10.4172/2155-952X.S3-001.
(24) Li L, Duan X, Fan ZX, Chen L, Xing F, Xu Z, et al. Mesenchymal stem cells in combination with hyaluronic acid for articular cartilage defects. Sci Rep. 2018;8(1):1–11. doi: 10.1038/s41598-018-27737-y.
(25) Koh RH, Jin Y, Kim J, Hwang NS. Inflammation-modulating hydrogels for osteoarthritis cartilage tissue engineering. Cells. 2020;9(419):1–17. doi: 10.3390/cells9020419.
(26) Ito T, Yeo Y, Highley CB, Bellas E, Benitez CA, Kohane DS. The prevention of peritoneal adhesions by in situ cross-linking hydrogels of hyaluronic acid and cellulose derivatives. Biomaterials. 2007;28:975–83. doi: 10.1016/j.biomaterials.2006.10.021.
(27) Yeo Y, Highley CB, Bellas E, Ito T, Marini R, Langer R, et al. In situ cross-linkable hyaluronic acid hydrogels prevent post-operative abdominal adhesions in a rabbit model. Biomaterials. 2006;27:4698–705. doi: 10.1016/j.biomaterials.2006.04.043.
(28) Emoto S, Yamaguchi H, Kamei T, Ishigami H, Suhara T, Suzuki Y, et al. Intraperitoneal administration of cisplatin via an in situ cross-linkable hyaluronic acid-based hydrogel for peritoneal dissemination of gastric cancer. Surg Today. 2014;44:919–26. doi: 10.1007/s00595-013-0674-6.
(29) Hu MH, Yang KC, Sun YH, Chen YC, Yang SH, Lin FH. In situ forming oxidised hyaluronic acid/adipic acid dihydrazide hydrogel for prevention of epidural fibrosis after laminectomy. Eur Cell Mater. 2017;34:307–20. doi: 10.22203/eCM.v034a19.
(30) Smith BD, Grande DA. The current state of scaffolds for musculoskeletal regenerative applications. Nat Rev Rheumatol. 2015;11:213–22. doi: 10.1038/nrrheum.2015.27.
(31) Hsiao MY, Lin AC, Liao WH, Wang TG, Hsu CH, Chen WS, et al. Drug-loaded hyaluronic acid hydrogel as a sustained-release regimen with dual effects in early intervention of tendinopathy. Sci Rep. 2019;9(1):1–9. doi: 10.1038/s41598-019-41410-y.
(32) Lai JY, Ma DHK. Ocular biocompatibility of gelatin microcarriers functionalized with oxidized hyaluronic acid. Mater Sci Eng C. 2017;72:150–9.
(33) Lai JY. Biofunctionalization of gelatin microcarrier with oxidized hyaluronic acid for corneal keratocyte cultivation. Colloids Surf B. 2014;122:277–86.
(34) França CG, Plaza T, Naveas N, Santana MHA, Manso-Silvan M, Recio G, et al. Nanoporous silicon microparticles embedded into oxidized hyaluronic acid/adipic acid dihydrazide hydrogel for enhanced controlled drug delivery. Micropor Mesopor Mat. 2021;310(110634):1–11. doi: 10.1016/j.micromeso.2020.110634.

(35) Ma XB, Xu TT, Chen W, Wang R, Xu Z, Ye ZW, et al. Improvement of toughness for the hyaluronic acid and adipic acid dihydrazide hydrogel by PEG. Fiber Polym. 2017;18:817–24. doi: 10.1007/s12221-017-6986-1.
(36) Zu Y, Zhang Y, Zhao X, Shan C, Zu S, Wang K, et al. Preparation and characterization of chitosan–polyvinyl alcohol blend hydrogels for the controlled release of nano-insulin. Int J Biol Macromol. 2012;50:82–7. doi: 10.1016/j.ijbiomac.2011.10.006.
(37) Mosmann T. Rapid colorimetric assay for cellular growth and survival: application to proliferation and cytotoxicity assays. J lmmunol Methods. 1983;65:55–63. doi: 10.1016/0022-1759(83)90303-4.
(38) Jensen C, Teng Y. Is it time to start transitioning from 2D to 3D cell culture? Front Mol Biosci. 2020;7:33. doi: 10.3389/fmolb.2020.00033.
(39) Caliari SR, Burdick JA. A practical guide to hydrogels for cell culture. Nat Methods. 2016;13(5):405–14. doi: 10.1038/nmeth.3839.
(40) Cavalcanti ADD, Santana MHA. Structural and surface properties control the recovery and purity of bio-hyaluronic acid upon precipitation with isopropyl alcohol. Colloid Surf A Physicochem Eng Asp. 2019;573:112–8. doi: 10.1016/j.colsurfa.2019.04.027.
(41) Cacua K, Ordonez F, Zapata C, Herrera B, Pabon E, Buitrago-Sierra R. Surfactant concentration and pH effects on the zeta potential values of alumina nanofluids to inspect stability. Colloid Surf A Physicochem Eng Asp. 2019;583(123960):112–8. doi: 10.1016/j.colsurfa.2019.123960.
(42) Shimojo AAM, Pires AMB, de la Torre LG, Santana MHA. Influence of particle size and fluid fraction on rheological and extrusion properties of crosslinked hyaluronic acid hydrogel dispersions. J Appl Polym Sci. 2013;128:2180–5. doi: 10.1002/app.38389.
(43) Kablik J, Monheit GD, Yu LP, Chang G, Gershkovich J. Comparative physical properties of hyaluronic acid dermal fillers. Dermatol Surg. 2009;35:302–12. doi: 10.1111/j.1524-4725.2008.01046.x.
(44) Sheu SY, Chen WS, Sun JS, Lin FH, Wu T. Biological characterization of oxidized hyaluronic acid/resveratrol hydrogel for cartilage tissue engineering. J Biomed Mater Res A. 2013;101(12):3457–66. doi: 10.1002/jbm.a.34653.
(45) Declercq H, De Caluwe T, Krysko O, Bachert C, Cornelissen M. Bone grafts engineered from human adipose-derived stem cells in dynamic 3d-environments: a top-down versus bottom-up approach. J Tissue Eng Regen Med. 2012;6:23–4.